Interdisciplinary Research in Medical Sciences Specialty
ISSN: 3062-4401
2026, Volume 6, Issue 1, Page No: 299-319

Available online at: www.galaxypub.co/page/journals

Galaxy Publication

Dimethyl Itaconate Attenuates Dendritic Cell and CD8+ T Cell Responses to Prevent Vitiligo Progression

Lina Hassan[1]*, Omar Khalaf[2], Reem Jaber[1], Rania Mostafa[3]

[1]Department of Dermatology and Autoimmune Skin Diseases, Faculty of Medicine, University of Jordan, Amman, Jordan.
[2]Department of Dendritic Cell Biology and T Cell Responses, Faculty of Medicine, Jordan University of Science and Technology, Irbid, Jordan.
[3]Department of Vitiligo Research and Immunomodulation, Faculty of Medicine, Al-Balqa Applied University, Salt, Jordan.

***E-mail** ✉ lina.hassan@ju.edu.jo

Received: 29 April 2026; **Revised:** 22 June 2026; **Accepted:** 24 June 2026

ABSTRACT

Although autoimmunity driven by dendritic cells (DCs) and CD8+ T cells plays a central role in the destruction of melanocytes during vitiligo, effective treatments are scarce due to the lack of approaches that simultaneously address both cell populations. We investigated the link between the immunoregulatory metabolite itaconate and vitiligo progression by measuring serum itaconate concentrations in patients with vitiligo and tracking depigmentation in Acod1 knockout (KO) mice, which lack endogenous itaconate production. We then tested the therapeutic potential of the itaconate derivative dimethyl itaconate (DI) in mouse models of the disease and examined its impact on the recruitment and functional activity of cutaneous DCs and CD8+ T cells both in vivo and ex vivo. Gene expression profiles and involved signaling pathways were also analyzed in DI-exposed CD8+ T cells. Patients with vitiligo displayed increased levels of circulating itaconate. In contrast, itaconate deficiency in Acod1 KO mice led to faster depigmentation following disease induction. Treatment with DI effectively prevented vitiligo progression and supported repigmentation, accompanied by higher systemic itaconate, greater melanocyte numbers, and lower densities of skin-infiltrating CD8+ T cells. At the cellular level, DI suppressed CD8+ T cell activation (CD69), effector cytokine production (IFN-γ), cytotoxic capacity (Gzmb), proliferation, and expression of proinflammatory genes (Csf1, Ifitm1, CD49a, NKG2D, and NKG2A), at least in part through inhibition of the JAK–STAT signaling pathway. Additionally, DI reduced the infiltration of DCs into the skin and decreased the proportion of DCs exhibiting mature and migratory characteristics. These results highlight DI as a small-molecule derivative of an endogenous metabolite that safeguards against autoimmune damage by simultaneously modulating DC and CD8+ T cell responses. This dual-targeting mechanism offers a compelling therapeutic avenue for vitiligo and potentially other organ-specific autoimmune conditions.

Keywords: Autoimmune disease, CD8+ T cell, Dendritic cell, Dimethyl itaconate, JAK-STAT pathway, Vitiligo

How to Cite This Article: Hassan L, Khalaf O, Jaber R, Mostafa R. Dimethyl Itaconate Attenuates Dendritic Cell and CD8+ T Cell Responses to Prevent Vitiligo Progression. Interdiscip Res Med Sci Spec. 2026;6(1):299-319. https://doi.org/10.51847/WeCotfQjVi

Introduction

Vitiligo represents a classic autoimmune skin disorder marked by progressive, treatment-resistant depigmentation that affects 0.5%–2% of people globally [1-4]. It is widely accepted that autoreactive CD8+ T cells serve as the primary mediators of disease development [1-3]. This concept originated from initial findings showing heavy $CD8^+$ T cell accumulation in the dermis and epidermis of perilesional areas, along with the ability of melanocyte-targeted cytotoxic $CD8^+$ T cells to destroy melanocytes in laboratory settings [1, 5, 6]. In vitiligo lesions, IFN-γ released by $CD8^+$ T cells stimulates nearby keratinocytes and fibroblasts to produce chemokines through the IFN-γ receptor-Janus kinase (JAK) signaling cascade. This process creates a self-perpetuating inflammatory cycle that draws in additional CD8+ T cells [1]. Multiple recent clinical studies have shown that JAK inhibitors (JAKi),

which interrupt this IFN-γ–chemokine pathway and thereby limit CD8+ T cell recruitment, produce positive therapeutic outcomes [7, 8]. These results underscore the value of addressing the CD8+ T cell-driven autoimmune process in vitiligo management.

Dendritic cells (DCs) act as key upstream controllers that direct melanocyte-specific $CD8^+$ T cell immunity in vitiligo through antigen cross-presentation and priming of $CD8^+$ T cells within the dermis [9]. Furthermore, vitiligo patients exhibit higher DC counts and elevated proinflammatory cytokines from DCs in both blood and perilesional skin [10-12]. Supporting data from animal studies demonstrate vitiligo onset following transfer of premelanosome protein (PMEL)-loaded dendritic cells together with PMEL-specific CD8+ T cells [13, 14]. Blocking DC activity [12] has proven highly effective in murine vitiligo models. Nevertheless, DC suppression by itself is insufficient to control already activated CD8+ T cells, while direct CD8+ T cell inhibition does not stop ongoing DC-mediated priming that maintains T cell activity. Therefore, combined approaches that simultaneously modulate DC and CD8+ T cell adaptive immune responses are essential for stronger suppression of autoimmunity, yet such strategies remain undeveloped for vitiligo.

Growing awareness of metabolites that possess immune-modulating capabilities is transforming approaches to autoimmune disease therapy [15]. Itaconate is generated in activated macrophages during metabolic shifts via decarboxylation of cis-aconitate by the enzyme cis-aconitate decarboxylase 1 (Acod1, also called immune-responsive gene 1 or Irg1) [16, 17]. In clinical settings, raised endogenous itaconate concentrations occur during early sepsis [18], indicating its potential function as a metabolic modulator of autoimmune and inflammatory conditions and as a possible indicator of disease activity. Itaconate exhibits strong anti-inflammatory actions. To explore its pathways, investigators frequently employ membrane-permeable ester forms such as dimethyl itaconate (DI) or 4-octyl itaconate (OI) [17, 19]. Research with these compounds reveals that itaconate curbs inflammation by engaging the nuclear factor erythroid-2 related factor 2 (Nrf2) pathway [20], blocking inflammasome assembly [21], and inhibiting the NF-κB pathway [22] in macrophages. Administration of itaconate or its analogs has reduced immune activity in models of macrophage-associated autoimmune and inflammatory disorders [17, 23]. Importantly, although these derivatives mimic itaconate structurally, emerging evidence suggests they do not always replicate its full biological impact, emphasizing the importance of clear differentiation [19]. Considering its robust anti-inflammatory capabilities, we examined whether itaconate or its derivatives might limit autoimmune progression in vitiligo by concurrently affecting DC and CD8+ T cell activities.

To explore the contributions of itaconate and its derivative DI to vitiligo onset and therapy, we utilized complementary approaches involving Acod1 gene deficiency and DI administration in mice, followed by analysis of DI's influence on skin infiltration and activity of dendritic cells and CD8+ T cells in living animals and isolated cell cultures.

Materials and Methods

Participant enrollment

Individuals with a clinical diagnosis of active or stable vitiligo were recruited from the Department of Dermatology at Xijing Hospital, Fourth Military Medical University. Patients were assigned to the active vitiligo category if they met any of these conditions: 1) appearance of new lesions or clear expansion of existing ones in the previous 6 months [24], 2) Koebner's phenomenon, 3) confetti-like depigmentation, or 4) trichrome sign [25, 26]. Patients whose lesions showed no change for over 6 months were included in the stable group to confirm disease stability [24]. Exclusion criteria encompassed any history of other inflammatory, autoimmune, or infectious illnesses, as well as use of topical or systemic treatments or narrow band-UVB therapy in the 3 months before sample collection. Age- and sex-matched healthy controls were enrolled from the Health Management Center of Xijing Hospital.

Animals and animal care

C57BL/6 mice were obtained from Hunan Slaccas Laboratory Animal Company. Acod1 homozygous knockout (Acod1 KO) mice were produced by breeding C57BL/6 N-Acod1em1cyagen (Acod1±, stock no. KOCMP-16365-Acod1-B6N-VA) mice acquired from Cyagen Biosciences. Genotyping of Acod1 KO mice and their wild-type littermates was performed using primers F1-TGTTACAGTCAGAGATGGAGAGG, R1-CACACACAGCAGCTCACAGTAG, and R2-TGTGTCAGGTACGGTAATGAGTG with PCR conditions: 94 °C for 3 min; followed by 33 cycles of 94 °C for 30 s, 62 °C for 35 s, 72 °C for 35 s; and a final extension at 72

°C for 5 min. Products were separated on 2% agarose gels (Sigma-Aldrich), producing a 670 bp band for homozygous knockouts, a 464 bp band for wild-type, and both bands for heterozygotes. KRT14-Kitl4XTG2Bjl mice (Krt14-Kitl, also known as stem cell factor (SCF) transgenic mice) and PMEL T cell receptor (TCR) transgenic mice were sourced from The Jackson Laboratory. All animals were maintained in the laboratory animal facility of Fourth Military Medical University under specific pathogen-free conditions with free access to food and water, on a 12-h light–dark cycle at 22–25 °C and 50–55% humidity. Littermates of matching sex or same-batch purchased mice were randomly allocated to study groups.

Induction of vitiligo in mice

Two established vitiligo models were employed to assess the impact of itaconate derivatives on disease progression and repigmentation. The melanoma-associated vitiligo model was generated following previously published protocols [4, 27, 28]. This approach mirrors human vitiligo by combining B16F10 melanoma cell injection, surgical tumor removal, and CD4+ Treg depletion to activate host autoreactive cytotoxic CD8+ T cells against melanocytes. Briefly, 6–8-week-old mice received intradermal injection of 2×10^5 B16F10 melanoma cells into the left flank on day 0. CD4-depleting antibodies (200 μg per 20 g body weight) were administered intraperitoneally on days 4 and 10. Primary tumors were excised surgically on day 12. No spontaneous metastases were detected, and animals with tumor regrowth after surgery (< 2%) were removed from the study. Five weeks after induction, vitiligo development was evaluated by whole-mount immunofluorescence staining of tail epidermis to count melanocytes and CD8+ T cells. Mice that developed vitiligo (roughly 75% as reported previously [28]) and showed CD8+ T cell infiltration in tail epidermis [4, 28, 29] were selected for further experiments. Non-induced mice served as controls, and animals with confirmed vitiligo were randomly divided into treatment or vehicle groups. Tail skin was chosen for assessment because melanocytes reside in both the epidermis and hair follicles there, closely resembling human skin, unlike dorsal skin where they are confined to hair follicles [4]. Tail depigmentation thus served as the primary indicator of vitiligo.

The adoptive transfer vitiligo model was established as described earlier [30]. Naïve CD8+ T cells from PMEL TCR transgenic mouse spleens were isolated by magnetic negative selection (Miltenyi Biotec). These purified cells (10^6 per recipient) were injected retro-orbitally into 10–12-week-old SCF transgenic hosts. One day prior to transfer, recipient mice received sublethal γ-irradiation (5.192 Gy) and were given an intraperitoneal injection of 1×10^6 pfu recombinant vaccinia virus expressing PMEL antigen (Genechem) on the day of T cell transfer.

In vivo treatment experiments

Mice in the established vitiligo model received intraperitoneal injections starting five weeks after melanoma cell implantation. Each animal was given 20 mg of dimethyl itaconate (DI; Sigma Aldrich) suspended in 400 μl of sterile phosphate-buffered saline (PBS), or 50 mg/kg of 4-octyl itaconate (OI; MedChemExpress) formulated in 40% hydroxypropyl-beta-cyclodextrin dissolved in PBS, or PBS alone as the control. These treatments were administered five days per week over five successive weeks. Following completion of the treatment course, animals were euthanized, and tissues including spleen, draining lymph nodes, peripheral blood, and tail skin were collected for flow cytometry assessments. Serum samples were isolated to quantify circulating itaconate levels. To eliminate bias, both sample harvesting and subsequent data interpretation were conducted in a blinded manner, with investigators and analysts unaware of the treatment assignments.

For long-term repigmentation evaluation, mice with SCF-driven vitiligo (induced 24 weeks prior) underwent intraperitoneal DI administration at 20 mg per mouse, five times weekly, continuing for a full 24 weeks. Tail skin pigmentation status was documented with photographs at designated time points, and the surface area of depigmented regions was measured quantitatively using ImageJ software.

Preparation of human peripheral blood mononuclear cells (PBMCs) and serum samples

PBMCs were separated from 30 mL venous blood samples obtained from individuals with active vitiligo or matched healthy donors employing Lymphoprep density gradient medium (Dakewe) as outlined by the supplier. Serum fractions were generated by spinning fresh whole blood from human subjects or experimental mice at 2500 rpm for 5 minutes at 4 °C, followed by rapid freezing in liquid nitrogen. All serum specimens were kept at −80 °C for long-term storage. Immediately prior to experimental use, samples were shifted to −20 °C for 20 minutes and subsequently thawed gradually on ice to preserve integrity and limit breakdown.

Preparation of murine single cell suspensions

Excised tail skin specimens underwent initial enzymatic digestion using Dispase II solution (2.5 mg/ml, Sigma Aldrich) for 1 hour at 37 °C. The epidermal layer was carefully detached and gently disrupted by passage through a 40 μm cell strainer (BD Falcon). The underlying dermal tissue was further processed with collagenase IV (1 mg/ml, Sigma Aldrich) combined with deoxyribonuclease I (2 mg/ml, Sigma Aldrich) for 1 hour at 37 °C, then mechanically dissociated using the same 40 μm strainer. Skin-draining lymph nodes and spleens were dissociated by physical disruption across 70 μm filters. Erythrocytes present in spleen cell preparations were eliminated with ACK lysis buffer (Thermo Fisher Scientific). Final cell suspensions were filtered twice to ensure high-purity single-cell isolates.

Cell culture, stimulation, and treatment

B16F10 melanoma cells (ATCC CRL-6475) were propagated in high-glucose DMEM (Gibco) enriched with 10% fetal bovine serum (Pricella) and 1% penicillin-streptomycin mixture (Solarbio) for short-term use in in vivo tumor induction. All other primary and cell line cultures were grown in RPMI-1640 base medium containing 10% FBS and 1% penicillin-streptomycin, with adjustments tailored to individual assay requirements. Human PBMCs, murine splenocytes, lymph node-derived cells, and skin cell isolates were plated at densities of $1–2 \times 10^6$ cells per mL in 24- or 96-well formats for functional testing. THP-1 monocytic cells were first differentiated into macrophages and then placed in Transwell inserts for co-culture assays involving T lymphocytes.

Optimal DI dosing for ex vivo work [22] was established by exposing PBMCs from active vitiligo patients and splenocytes from disease-model mice to a range of DI concentrations for three days, after which viability was evaluated by CCK-8 assay following the vendor's guidelines (7 Sea Biotech). A concentration of 250 μM DI was selected for the majority of follow-up experiments unless specified differently.

DC maturation status was investigated by pre-incubating whole blood from vitiligo patients with DI for 18 hours prior to an 8-hour challenge with 1 μg/mL lipopolysaccharide (LPS; Thermo Fisher). Erythrocytes were subsequently lysed using ACK buffer (Thermo Fisher) before proceeding to flow cytometry.

IL-12 secretion by DCs was quantified after pre-treating lymph node cell suspensions with DI for 18 hours (seeded at 2×10^6 cells in 500 μL medium per well), followed by combined stimulation with 10 ng/mL IFN-γ (BioLegend) and 1 μg/mL LPS for 16 hours. Brefeldin A (eBioscience) was included during the terminal 6 hours to retain intracellular cytokines for flow cytometric detection.

Assessment of CD8+ T cell activation markers and cytokine release involved pretreating PBMCs, skin-derived single cells, or mouse splenocytes with DI for 18 hours, then activating them either with a commercial cell stimulation cocktail (Cat#423304, BioLegend) for 6 hours or anti-human CD3/CD28 beads (T&L Biological Technology) for 24 hours. To examine direct actions on CD8+ T cells specifically, these lymphocytes were positively selected from patient PBMCs with a CD8a+ T Cell Isolation Kit (Miltenyi Biotec) per manufacturer instructions. Parallel comparisons included treatment with 0.25 or 5 mM itaconate (GLPBIO), 0.05 mM dimethyl fumarate (GLPBIO), and 7.5 mM sulforaphane (GLPBIO), all prepared according to established methods [19, 22, 31]. Treated PBMCs underwent 18-hour compound exposure, 6-hour activation, and subsequent flow analysis.

Purified human $CD8^+$ T cells (isolated via Miltenyi magnetic beads) were used to study STAT signaling. Cells received DI pretreatment for 16–24 hours, followed by stimulation with anti-CD3/CD28 beads plus 100 ng/mL IL-2 (PeproTech) for 30 minutes to evaluate phosphorylation, or extended stimulation (1–2 hours) for Western blotting of total STAT proteins. JAK phosphorylation was measured after 10 minutes of stimulation in similarly pretreated cells.

Flow cytometry

Viability staining was performed with Zombie Fixable Viability Dye (BioLegend) to gate out non-viable cells. Nonspecific binding was prevented by 15-minute room-temperature incubation with TruStain FcX blocking reagent (anti-mouse or anti-human CD16/32; BioLegend). Surface antigens on DCs, CD8+ T cells, and macrophages were labeled for 30 minutes at 4 °C using fluorophore-conjugated antibodies (BioLegend unless noted). The panel included mouse antibodies targeting CD45 (I3/2.3), CD3 (145-2C11), CD11c (N418), CD11b (M1/70), CCR7 (4B12), MHCII (M5/114.15.2, eBioscience), CD80 (16-10A1), CD86 (GL-1), CD8a (53-6.7), CD69 (H1.2F3), NKG2AB6 (16A11), CD49a (HMα1), and F4/80 (QA17A29); and human antibodies for CD11c (3.9), CD11b (M1/70), CD14 (HCD14), CD15 (W6D3), CD16 (3G8), CD56 (MEM188), CD68 (Y1/82A), CD80 (W17149D), CD86 (BU63), HLA-DR (L243), CD8a (RPA-T8), and CD69 (FN50).

Intracellular proteins were detected after fixation/permeabilization with the FOXP3/Transcription Factor Buffer Set (eBioscience) using antibodies specific for mouse IFN-γ (XMG1.2), human IFN-γ (4S.B3), granzyme B

(QA16A02 for human/mouse), and CD68 (Y1/82A, Elabscience). Acquisition occurred on a BD LSR Fortessa cytometer, with data processed in FlowJo (Tree Star).

For phosphoprotein analysis, cells were fixed in 2% paraformaldehyde for 15 min at 37 °C, permeabilized in 90% ice-cold methanol for 30 min, and stained for CD8 together with phospho-STAT1 (A15158B), phospho-STAT3 (13A3-1), and phospho-STAT5 (SRBCZX, eBioscience). All analyses were restricted to live singlet populations, with appropriate isotype controls defining gate boundaries.

Macrophage and T-cell coculture

Co-culture experiments utilized a 0.4 μm pore Transwell system (Corning, 24-well format). THP-1 cells (1×10^6 per well) — either wild-type or Acod1 knockout variants (Cyagen SKO-1356-1B12) — were differentiated into M0 macrophages in the bottom compartment by 24-hour exposure to 100 ng/mL phorbol 12-myristate 13-acetate (PMA) at 37 °C in 5% CO_2. Polarization toward the M1 state and itaconate synthesis were induced by subsequent 24-hour treatment with 20 ng/mL IFN-γ plus 100 ng/mL LPS. In selected rescue conditions, Acod1 KO macrophages received supplemental 5 mM itaconate during this polarization phase. Following polarization, 2 × 10^6 pre-activated $CD8^+$ T cells (stimulated for 24 hours with CD3/CD28 antibodies) were introduced into the upper chamber insert for 24-hour co-incubation. At the conclusion, $CD8^+$ T cells were recovered from the insert for flow cytometric characterization.

Whole-mount immunofluorescence

Tail skin tissues harvested from vitiligo mice across experimental conditions (pre- and post-treatment) were processed as whole mounts. Epidermis-dermis separation was achieved with 20 mM EDTA incubation. Epidermal sheets were cleared of sebaceous glands using a stereomicroscope, fixed briefly in 4% paraformaldehyde (10 min), rinsed, treated with 0.3% hydrogen peroxide in methanol (20 min at −20 °C), washed in PBS, and blocked for 1 hour (2% donkey serum, 1% bovine serum albumin, 0.3% Triton X-100 in PBS). Overnight incubation at 4 °C was performed with primary antibodies to CD8 (Abcam ab22378, 1:200) and MelanA (Abcam ab210546, 1:200). After thorough washing, secondary antibodies and DAPI (1:1000) were applied for 8 hours at 4 °C. Samples were mounted in 50% glycerol and visualized on a Zeiss LSM 880 confocal microscope using a 10× objective. Z-stack images (512 × 512 resolution) were captured and quantified following previously reported protocols [4] with Imaris 3D analysis software (Bitplane).

Determination of itaconate by liquid chromatograph–mass spectrometer (LC–MS)

A comprehensive description of the LC-MS protocol used for itaconate quantification is available in Additional file 1: Supplementary methods.

RNA-seq analysis

Purified CD8+ T cells underwent bulk RNA sequencing. These cells were isolated magnetically (Cat#130-117-044, Miltenyi Biotec) from skin-draining lymph nodes of wild-type mice as well as PBS- or DI-treated vitiligo animals at the 11-week time point. RNA extraction was carried out with TRIzol reagent (Invitrogen). Sequencing libraries were prepared and run on the DNBSEQ platform (BGI-NGS-JK-RNA-007 A0, BGI Genomics). Data processing and analysis were conducted using the BGI Dr.Tom online platform (https://biosys.bgi.com/#/report/login). Differentially expressed genes were identified with the DEGseq algorithm, applying cutoffs of log2 fold change greater than 1 and false discovery rate below 0.05.

Publicly available single-cell RNA-seq datasets from vitiligo patient skin [4, 32] and peripheral blood [33, 34] were re-examined through the Omicsmart interactive web tool.

Western blot analysis

Human CD8+ T cells isolated by magnetic selection were lysed in RIPA buffer supplemented with 2% protease inhibitor cocktail (Roche) and boiled at 95 °C for 5 minutes. Lysates were clarified by centrifugation at 14,000 rpm for 10 minutes at 4 °C, after which supernatants were used for electrophoresis. Proteins were separated on 8% SDS-PAGE gels and transferred to polyvinylidene difluoride membranes using a wet transfer apparatus. Membranes were blocked with 5% (w/v) non-fat dry milk in TBS-Tween for 1 hour at room temperature. Primary antibodies were applied at 1:1000 dilution overnight at 4 °C, followed by incubation with appropriate horseradish peroxidase-linked secondary antibodies. The primary antibodies included anti-p-JAK1 (Abcam, Cat#138005), anti-JAK1 (Proteintech, Cat#66466-1-Ig), anti-p-JAK2 (Cell Signaling Technology, Cat#3776), anti-JAK2 (Cell

Signaling Technology, Cat#3230), anti-p-JAK3 (Cell Signaling Technology, Cat#5031), anti-JAK3 (Cell Signaling Technology, Cat#8827), anti-p-STAT1 (Cell Signaling Technology, Cat#7649), anti-STAT1 (Cell Signaling Technology, Cat#14994), anti-p-STAT3 (Cell Signaling Technology, Cat#9145), anti-STAT3 (Cell Signaling Technology, Cat#9139), and anti-β-actin (Proteintech, Cat#66009-1-Ig, used at 1:20,000). After imaging phosphorylated proteins, membranes were stripped using PVDF Stripping Buffer (CoWin Biosciences, Cat#CW0056M) and re-probed for the corresponding total proteins. β-actin served as the loading control for both phosphorylated and total protein forms on the same membrane. Signal detection was achieved with enhanced chemiluminescence reagents using a Bio-Rad imaging system.

CFSE cell proliferation assay

Fresh human PBMCs were suspended at 1×10^6 cells/mL in PBS and labeled with CFSE (BioLegend). Labeled cells were washed and plated at 2×10^5 cells per 200 μL in 96-well round-bottom plates. Cultures were treated with DI and/or stimulated using anti-human CD3/CD28 beads at 37 °C under 5% CO2 conditions. After 5 days, cells were collected, stained with anti-CD8 antibody (BioLegend) and Zombie Fixable Viability Dye (BioLegend) for 30 minutes at 4 °C, and analyzed by flow cytometry.

Enzyme linked immunosorbent assay (ELISA)

Murine serum IL-12 levels were quantified using Quantikine ELISA kits according to the manufacturer's protocol (Elabscience). Absorbance was read at 450 nm on a microplate reader (Thermo Fisher).

Statistics

All ex vivo experiments were repeated at least three times independently, while in vivo studies were performed at least twice. Statistical evaluations were conducted in GraphPad Prism 8. Data are presented as median with interquartile range (25th–75th percentiles), mean ± SEM, or mean ± SD. Comparisons between two groups used unpaired Student's t-test. Analyses involving three or more groups employed Kruskal-Wallis H test, one-way ANOVA, or two-way ANOVA as appropriate. Significance levels are indicated as * $P < 0.05$, ** $P < 0.01$, *** $P < 0.001$, and **** $P < 0.0001$.

Results and Discussion

Endogenous itaconate deficiency worsens vitiligo development in mice

To explore the relationship between itaconate and vitiligo, circulating itaconate concentrations were measured in 38 patients. Levels were substantially elevated in both active and stable disease relative to healthy controls [0.057 (0.014–0.083) μM and 0.047 (0.032–0.058) μM versus 0.006 (0.005–0.010) μM, respectively] **(Figure 1a)**. No meaningful correlation was found between serum itaconate and disease severity as assessed by Vitiligo Area Scoring Index (VASI) or disease duration. Similarly, itaconate concentrations did not differ significantly across varying stages of disease activity.

A mouse model replicating key aspects of human vitiligo was generated through B16F10 melanoma cell implantation, regulatory T cell depletion, and subsequent tumor resection **(Figure 1b)**. In these animals, serum itaconate rose to higher levels [0.016 (0.012–0.021) μM] compared with non-induced controls [0.011 (0.006–0.014) μM] once visible depigmentation developed **(Figure 1c)**. Given that itaconate synthesis is primarily driven by Acod1 enzyme activity in activated macrophages [17], we investigated whether macrophages serve as the main source of elevated itaconate in vitiligo. Reanalysis of single-cell RNA sequencing data [4] showed increased expression of proinflammatory genes such as STAT1, CXCL10, CCL18, and S100A9 [35] in skin macrophages, consistent with their activated phenotype. Although Acod1 transcripts were not detected in patient skin lesions, low-level Acod1 expression was restricted to CD14+ monocytes (macrophage precursors) in circulating immune cells, without significant differences between patients and controls. Supporting this, patients displayed elevated numbers of CD14++CD16− classical monocytes and CD14++CD16+ intermediate monocytes. In addition, CD14+CD68+CD80+ macrophages (resembling classically activated M1-like proinflammatory macrophages) [36, 37] were increased in the blood of human vitiligo patients as well as in the skin-draining lymph nodes (F4/80+CD11b+) of vitiligo mice. Together, these observations indicate that itaconate production in vitiligo is likely macrophage-derived.

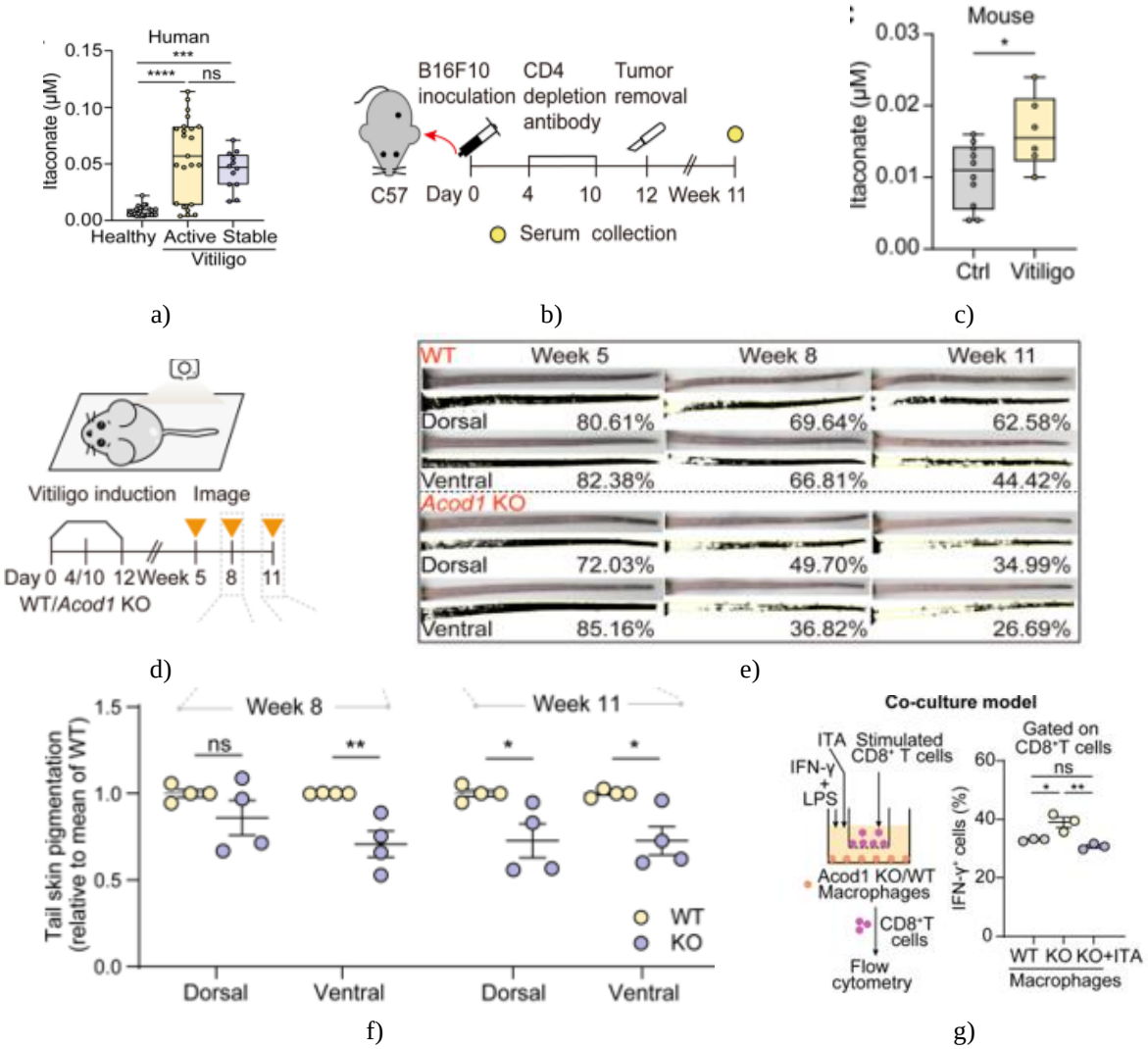

Figure 1. Absence of itaconate accelerates expansion of depigmented areas.

(a) Serum itaconate concentrations determined by targeted LC-MS in healthy individuals (n = 26), patients with active vitiligo (n = 23), and patients with stable disease (n = 12).
(b) Overview of the melanoma-associated vitiligo induction protocol in mice and schedule of serum collection.
(c) Serum itaconate levels measured by targeted LC-MS in non-induced control mice (n = 10) and vitiligo mice (n = 6).
(d) Schedule for tracking depigmentation progression in wild-type (WT) versus Acod1 knockout (KO) mice.
(e) Time-course photographs showing tail depigmentation in WT and Acod1 KO mice. Accompanying graph displays the percentage of pigmented area on dorsal and ventral tail surfaces.
(f) Quantification of dorsal and ventral tail pigmentation in Acod1 KO mice compared to WT controls at weeks 8 and 11 after vitiligo induction (n = 4 per group).
(g) WT or Acod1 KO THP-1 macrophages were polarized with LPS plus IFN-γ in Transwell chambers and subsequently co-cultured with $CD8^+$ T cells. Post-co-culture, $CD8^+$ T cells were collected for flow cytometric evaluation. In rescue conditions, 5 mM itaconate was added exogenously to Acod1 KO macrophages throughout the polarization step.
Box plots in panels A and C show median values with 25th–75th percentiles. Data in F and G represent mean ± SEM. Statistical analyses used Kruskal-Wallis H test (A), unpaired two-tailed Student's t-test (C, F), or one-way ANOVA followed by Tukey's multiple comparisons test (G). Experiments were independently repeated at least twice. ITA, itaconate. ns, not significant; * $P < 0.05$; ** $P < 0.01$; *** $P < 0.001$; **** $P < 0.0001$.
To assess itaconate's function in vitiligo under in vivo conditions, we created mice lacking endogenous itaconate production through complete Acod1 gene deletion [38] and applied the standard vitiligo induction protocol to these animals **(Figure 1d)**. Successful gene knockout was verified by PCR. Following induction, Acod1 KO mice

displayed markedly accelerated and intensified tail depigmentation relative to their wild-type (WT) counterparts **(Figure 1e)**. Depigmented regions were significantly larger on both dorsal and ventral aspects of the tail in knockout mice at weeks 8 and 11 post-induction **(Figure 1f)**. These findings establish that itaconate normally confers protection against vitiligo progression in living animals.

Given this evidence, we postulated that itaconate released by macrophages exerts its beneficial influence by restraining CD8+ T cell responses. This idea was tested in a Transwell co-culture setup pairing macrophages (either WT or Acod1 KO) with CD8+ T cells. T cells paired with Acod1 KO macrophages secreted substantially higher amounts of IFN-γ compared to those paired with WT macrophages. Supplementing the culture with itaconate during macrophage polarization completely prevented this heightened cytokine output **(Figure 1g)**. The results therefore confirm that itaconate originating from macrophages effectively limits CD8+ T cell effector activity.

Exogenous itaconate derivatives control and reverse vitiligo in mice

Owing to its highly polar nature and relatively low electrophilicity caused by the conjugated double bond, native itaconate exhibits limited ability to cross cell membranes [19]. As a result, cell-permeable ester derivatives are routinely utilized in functional studies of this metabolite [19]. To evaluate the therapeutic potential of such derivatives against vitiligo, DI or OI was administered to WT mice beginning at the stage when CD8+ T cells start infiltrating the epidermis, with PBS serving as control **(Figures 2a and 2b)**. Animals treated with either DI or OI showed delayed onset and reduced severity of tail depigmentation compared to the PBS group **(Figure 2c)**. Following six weeks of continuous treatment, pigmentation retention reached 77.30 ± 5.43% in the DI group and 75.1 ± 6.67% in the OI group, in contrast to only 52.94 ± 11.64% in vehicle-treated mice **(Figure 2d)**.

Whole-mount immunofluorescence examination of tail epidermis confirmed the disease-ameliorating effect, revealing preserved melanocyte numbers and notably lower infiltration of CD8+ T cells in DI- and OI-treated skin **(Figure 2e)**. These benefits likely stem from OI's conversion to free itaconate through hydrolysis [21] and DI's ability to stimulate endogenous itaconate production [39]. In agreement with this mechanism, serum itaconate concentrations were significantly elevated after DI or OI supplementation [0.057 (0.036–0.101) μM and 0.067 (0.030–0.083) μM, respectively] compared with the vehicle group [0.017 (0.010–0.018) μM] **(Figure 2f)**.

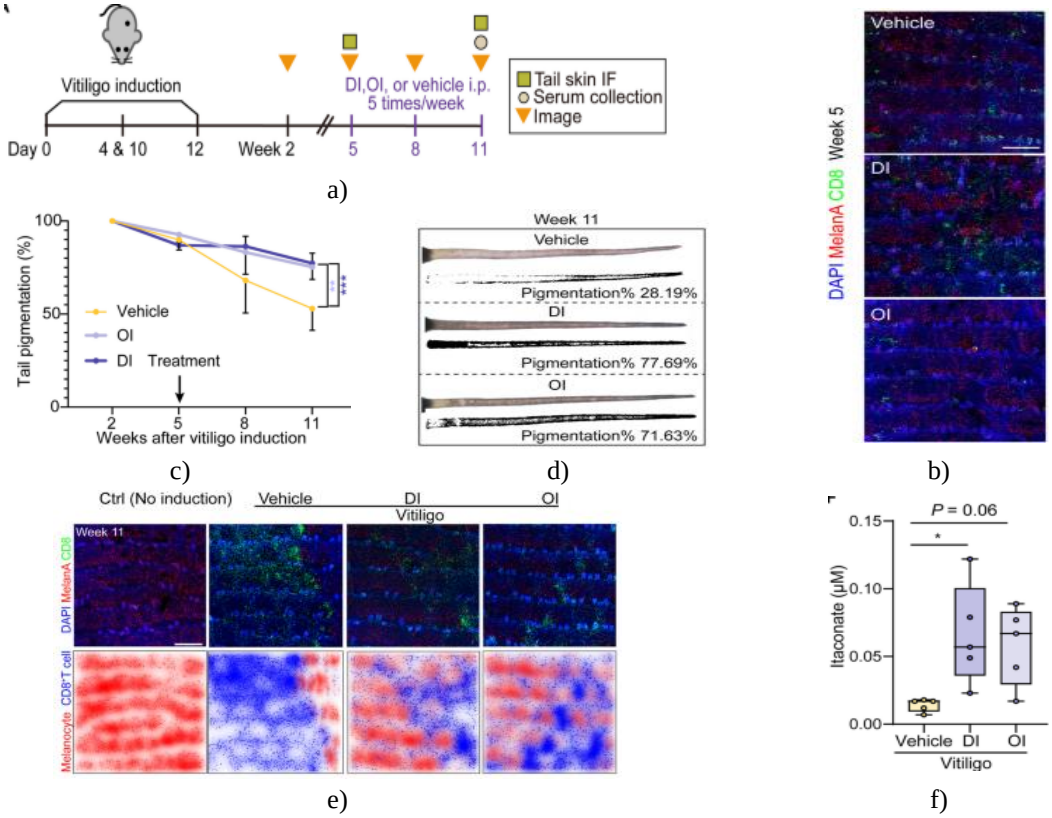

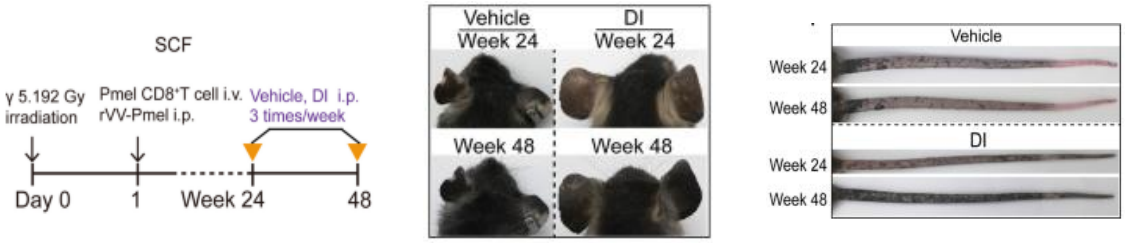

g) h) i)

Figure 2. Itaconate derivatives lessen depigmentation severity and drive repigmentation in experimental vitiligo.

(a) Overview of treatment protocols and timing of sample harvesting.
(b) Typical whole-mount immunofluorescence micrographs illustrating the presence of CD8+ T cells and melanocytes in the epidermis. Scale bar = 500 μm.
(c) Tail pigmentation percentages recorded at multiple time points. Statistical analysis by two-way ANOVA revealed a significant treatment effect ($P < 0.0001$) and time effect ($P = 0.0017$). Dunnett's test comparing treatments to vehicle yielded the following results marked with asterisks: DI vs vehicle at week 8 ($P = 0.0410$), OI vs vehicle at week 11 ($P = 0.1603$), DI vs vehicle at week 11 ($P = 0.0007$), and OI vs vehicle at week 11 ($P = 0.0020$).
(d) Photographs showing representative tail skin pigmentation in vehicle-, DI-, and OI-treated mice at week 11 after disease induction.
(e) Whole-mount immunofluorescence images (upper row) and density distribution plots (lower row) of tail epidermis from untreated controls, vehicle-, DI-, and OI-treated groups at week 11. Scale bar = 500 μm.
(f) Serum itaconate levels quantified by targeted LC-MS in vehicle-, DI-, and OI-treated vitiligo mice harvested at week 11.
(g) Schedule for vehicle or DI administration in the SCF transgenic mouse adoptive-transfer vitiligo model used for repigmentation assessment.
(h, i) Photographs of ear (H) and tail (I) skin in vehicle- versus DI-treated mice at weeks 24 and 48 post-induction. Values in panel C are expressed as mean ± SD; panel F data are shown as median (25th–75th percentiles). Findings are representative of a minimum of two independent experiments. i.p., intraperitoneal; IF, immunofluorescence; i.v., intravenous. ns, not significant; *$P < 0.05$; **$P < 0.01$; ***$P < 0.001$.

In vitiligo therapy, halting disease progression is important, yet restoring lost pigment remains a central clinical priority. To facilitate detailed evaluation of repigmentation, we employed an adoptive-transfer vitiligo model in SCF transgenic mice [30]. In this system, melanocytes populate both epidermal and follicular compartments **(Figure 2g)**. Due to its favorable solubility profile in PBS, only DI was used in the following long-term studies. Animals with established stable vitiligo (beyond 12 weeks post-induction) [30] were given intraperitoneal injections of DI three times per week over a 24-week period. This approach resulted in obvious pigment recovery in treated mice when compared with vehicle controls **(Figures 2h and 2i)**. Collectively, these data indicate that itaconate derivatives — most notably DI — can restrict further spread of white patches while actively encouraging the return of pigmentation.

DI suppresses CD8+ T cell-driven responses triggered by vitiligo in vivo

We next examined whether DI modulates CD8+ T cell activity by assessing cell numbers and cytokine output in treated vitiligo mice. Following the treatment period, DI administration led to a selective decrease in CD8+ T cell density within the tail epidermis, whereas populations in the dermis, skin-draining lymph nodes, spleen, and circulating blood remained comparable to controls **(Figures 3a and 3b)**.
Expression of the activation marker CD69 on CD8+ T cells was notably downregulated in the tail epidermis, dermis, spleen, and blood after DI exposure, although no change occurred in lymph nodes **(Figures 3c-3f)**. Moreover, IFN-γ production by CD8+ T cells was diminished in the epidermis and draining lymph nodes of DI-treated animals, while levels in the dermis and spleen were unaffected relative to vehicle-treated mice **(Figures 3g and 3h)**. These findings collectively demonstrate that DI reduces epidermal accumulation of CD8+ T cells and attenuates their activation state both at the local skin level and systemically.

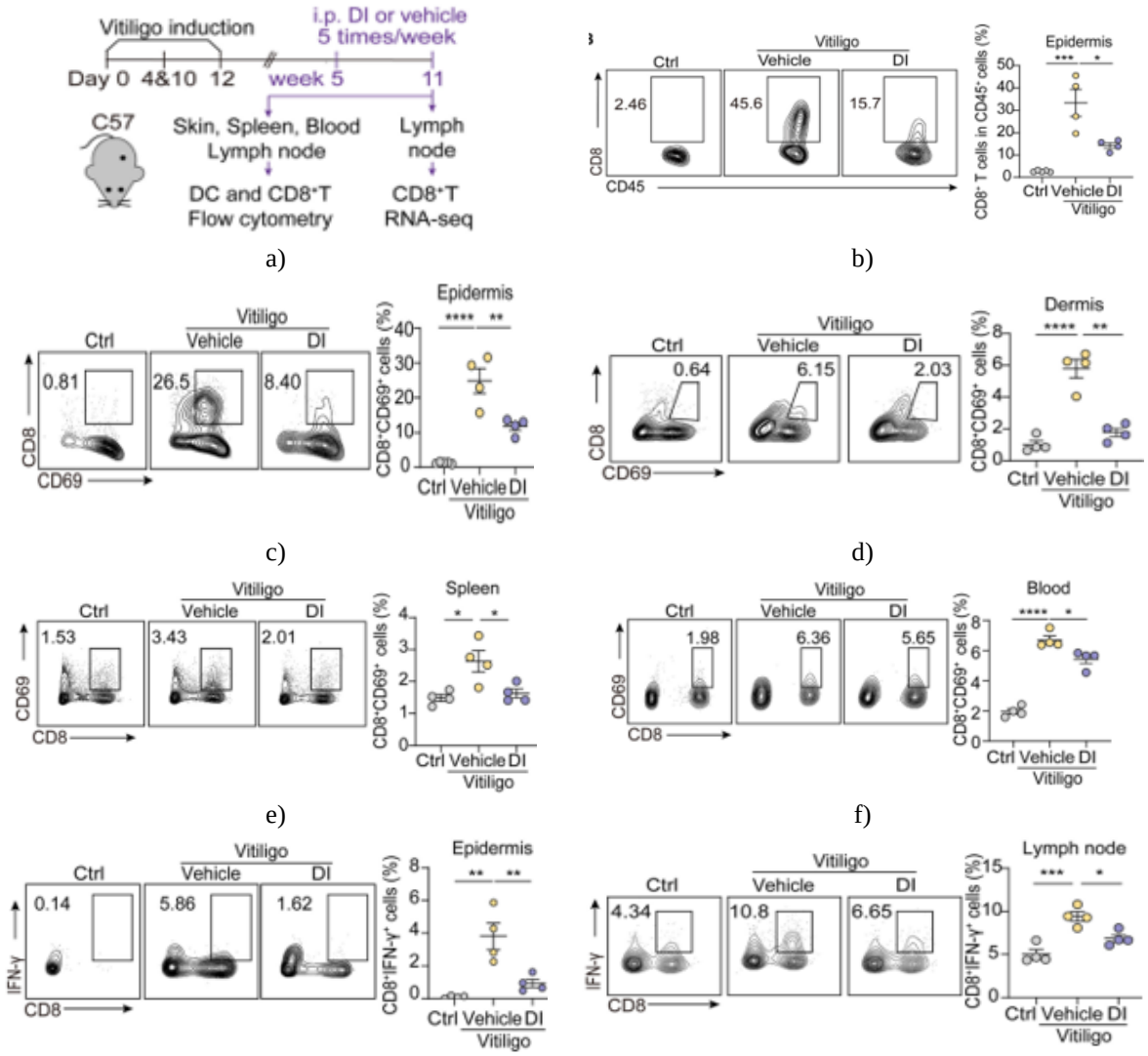

Figure 3. Treatment with DI lowers skin infiltration by CD8+ T cells and curbs their activation at both local and systemic sites.

(a) Schedule showing the timing of vehicle or DI injections in the vitiligo mouse model. Starting five weeks after induction, animals received 20 mg DI per mouse or PBS vehicle by intraperitoneal route, administered five days each week over six weeks.
(b) Flow cytometry example plots along with quantified percentages of CD8+ T cells within the CD45+ population in tail epidermis harvested at week 11 from untreated controls and from vitiligo mice given vehicle or DI.
(c–f) Example plots and statistical summary of CD8+CD69+ T cell proportions in tail epidermis (c), dermis (d), spleen (e), and peripheral blood (f) at week 11 in control, vehicle-treated, and DI-treated vitiligo groups.
(g–h) Measured frequencies of CD8+IFN-γ+ T cells via flow cytometry in epidermis (g) and skin-draining lymph nodes (h) of control mice versus vehicle- or DI-treated vitiligo mice at week 11.
All quantitative data are displayed as mean ± SEM. Statistical comparisons were performed by one-way ANOVA followed by Tukey's post-test (panels B–H). Experiments were repeated independently at least twice. * $P < 0.05$, ** $P < 0.01$, *** $P < 0.001$, **** $P < 0.0001$.

DI suppresses effector capabilities, cytotoxic potential, and proliferative activity of CD8+ T cells from vitiligo sources ex vivo

Additional experiments were performed to directly evaluate how DI affects the functional properties of CD8+ T cells. Lymphocytes derived from vitiligo mice and human patients were isolated and maintained in culture with or without DI supplementation. CD8+ T cells from mouse skin tissue and spleen were first stimulated using CD3/CD28 beads and then exposed to 250 μM DI, a dose previously confirmed as non-toxic to cell viability [22].

Under these conditions, DI markedly lowered IFN-γ release from both skin-derived (P = 0.034) and spleen-derived (P = 0.009) CD8+ T cells **(Figures 4a and 4b)**.

DI exposure did not significantly change Gzmb levels in skin CD8+ T cells **(Figure 4c)**, yet it reduced the fraction of skin cells co-expressing IFN-γ and Gzmb as well as the overall proportion of Gzmb-expressing CD8+ T cells in the spleen **(Figure 4d)**. Parallel studies using human cells from vitiligo patients revealed a clear dose-dependent decline in IFN-γ production upon DI treatment. Crucially, when CD8+ T cells were isolated prior to DI treatment, IFN-γ secretion was still inhibited, demonstrating direct action on this T cell subset **(Figure 4e)**. In matching human experiments, activated vitiligo CD8+ T cells displayed reduced Gzmb expression after DI incubation **(Figure 4f)**. DI further decreased the activation marker CD69 and strongly impaired proliferative responses in stimulated human vitiligo CD8+ T cells **(Figures 4g and 4h)**.

In summary, these observations solidly establish that DI exerts broad inhibitory effects on CD8+ T cells by limiting their effector cytokine output, cytotoxic granule components, activation state, and capacity to expand.

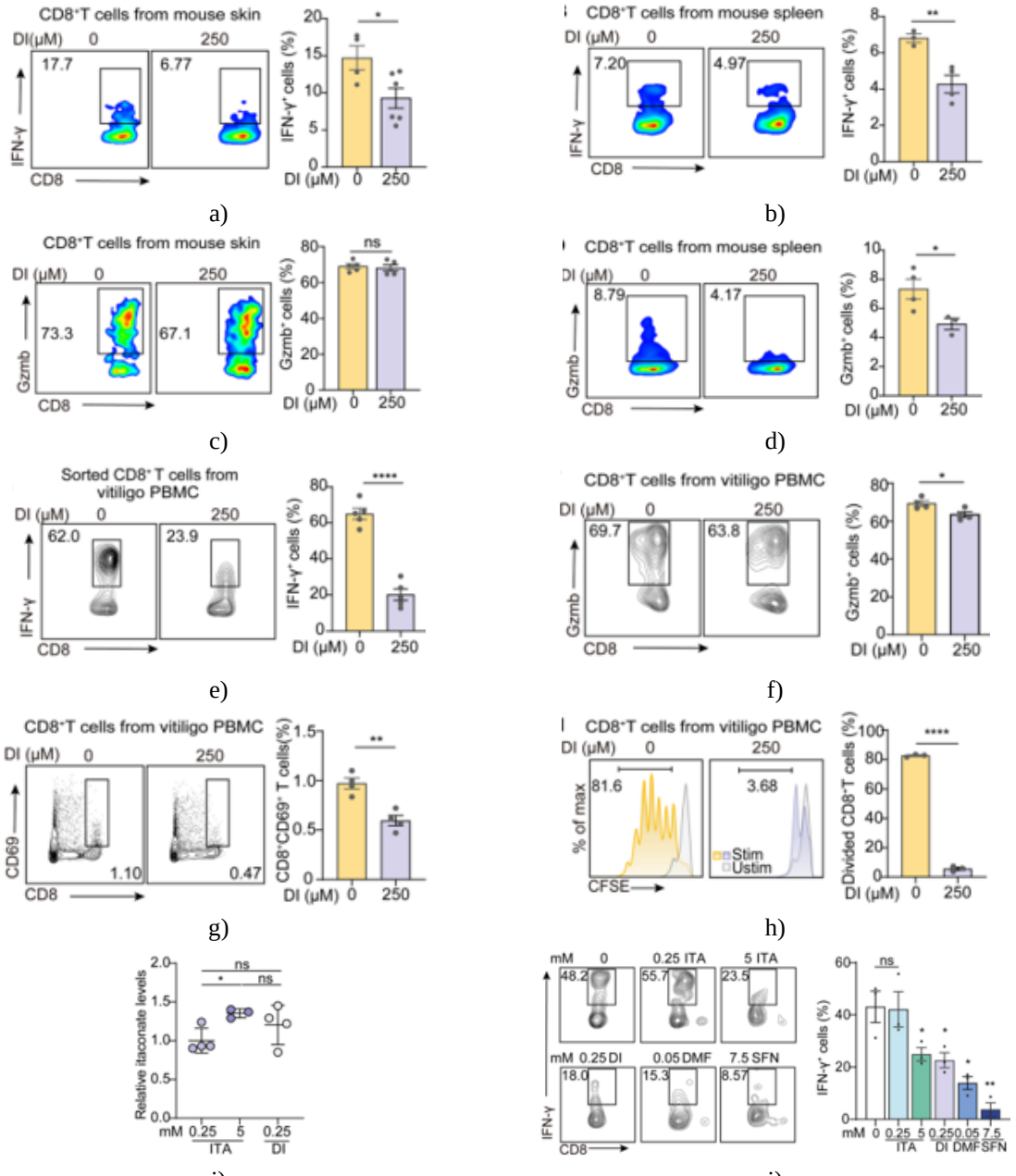

Figure 4. DI suppresses the effector function, cytotoxic activities, and proliferation of vitiligo CD8+ T cells ex vivo.

(a–b) Flow cytometry example plots and corresponding quantification of IFN-γ-positive CD8+ T cells derived from skin (a) and spleen (b) of vitiligo mice after an 18-hour incubation with or without 250 μM DI.
(c–d) Levels of Gzmb expression measured by flow cytometry in CD8+ T cells isolated from mouse skin (c) and spleen (d) following treatment with or without 250 μM DI.
(e–g) Representative flow plots and statistical analysis of IFN-γ production in purified CD8+ T cells (e), proportion of Gzmb-expressing CD8+ T cells (f), and CD69 levels (g) in CD8+ T cells from PBMCs of vitiligo patients treated with or without 250 μM DI for 18 hours.
(h) Example plots and quantification showing proliferation (cell division) of CD8+ T cells from vitiligo patients cultured with or without 250 μM DI and stimulated with anti-CD3/CD28 beads for 5 days.
(i) Intracellular itaconate concentrations (relative levels) in splenic CD8+ T cells measured after 3-hour exposure to 250 μM DI, 250 μM ITA, or 5 mM ITA.
(j) Frequency of IFN-γ-producing CD8+ T cells from vitiligo patient PBMCs following 18-hour treatment with 250 μM DI, 250 μM ITA, 5 mM ITA, 0.05 mM DMF, or 7.5 mM SFN.
Results are expressed as mean ± SEM. Comparisons were conducted using unpaired two-tailed Student's t-test (a–h, j) or one-way ANOVA with Tukey's post-hoc test (I). All data shown are representative of at least two independent experiments. ITA, itaconate; DMF, dimethyl fumarate; SFN, sulforaphane. ns, not significant; * $P < 0.05$, ** $P < 0.01$, **** $P < 0.0001$.

Given that DI does not undergo intracellular conversion to itaconate [39] and that authentic itaconate typically requires millimolar concentrations to elicit effects [19], we evaluated whether DI's suppressive impact on $CD8^+$ T cells occurs independently of itaconate and is instead linked to its electrophilic character. Incubation of $CD8^+$ T cells with 250 μM DI raised intracellular itaconate to levels comparable to 250 μM exogenous itaconate, both of which were markedly lower than those produced by 5 mM itaconate exposure **(Figure 4i)**. When tested in parallel, 250 μM DI, 5 mM itaconate, dimethyl fumarate, and sulforaphane all potently inhibited IFN-γ secretion, with the notable exception of 250 μM itaconate, which showed no significant effect **(Figure 4j)**. These experiments support the conclusion that DI exerts its inhibitory actions mainly via electrophilic properties rather than through generation of itaconate.

DI suppresses the JAK-STAT pathway, thereby impairing CD8+ T cell function

Further studies were undertaken to identify the intracellular signaling mechanisms responsible for DI's modulation of CD8+ T cells. Earlier reports indicated that itaconate stimulates Nrf2 and attenuates NF-κB activity in macrophages [20, 22]. Because these two pathways are also capable of influencing T cell responses [40, 41], we assessed DI's impact on Nrf2 and NF-κB in CD8+ T cells isolated from individuals with vitiligo. Interestingly, baseline Nrf2 protein abundance was already higher in vitiligo CD8+ T cells than in cells from healthy donors. Pretreatment with DI led to a further reduction in Nrf2 levels within activated vitiligo CD8+ T cells.
In agreement with these observations, application of the Nrf2 inhibitor ML385, the NF-κB activator TNF-α, or the non-canonical NF-κB stimulator AZD5582 did not counteract DI's ability to suppress IFN-γ production in vitiligo CD8+ T cells. Therefore, DI appears to limit CD8+ T cell activity through routes that do not involve Nrf2 upregulation or NF-κB blockade.
To gain broader insight, we performed bulk RNA sequencing on CD8+ T cells sorted from draining lymph nodes of vitiligo mice treated with either vehicle or DI **(Figure 3a)**. Pronounced transcriptional differences were detected between untreated controls and vehicle-treated vitiligo animals, as well as between vehicle- and DI-treated vitiligo groups **(Figures 5a and 5b)**. Vitiligo induction in vehicle-treated mice was associated with widespread upregulation of differentially expressed genes (DEGs) relative to controls **(Figures 5a and 5b)**. Intersection analysis revealed 992 genes that were overexpressed in vitiligo and subsequently downregulated by DI **(Figure 5c)**. Pathway enrichment analysis highlighted significant attenuation of the "cytokine-cytokine receptor interaction" and "T cell receptor signaling pathway" gene sets following DI treatment **(Figure 5d)**.
Since JAK-STAT signaling is central to cytokine-driven T cell responses through regulation of STAT phosphorylation [7, 42], we tested whether DI interferes with this cascade. Flow cytometry demonstrated that DI selectively decreased phosphorylation of STAT1 and STAT3 (but not STAT5) in human vitiligo CD8+ T cells **(Figure 5e)**. Western blot experiments confirmed lowered p-STAT1 and p-STAT3 protein levels in purified cells after DI exposure **(Figures 5f and 5g)**. Receptor ligation normally activates receptor-associated JAK kinases, leading to STAT phosphorylation and activation [43]. Analysis of these upstream kinases showed that DI specifically reduced JAK2 phosphorylation (p-JAK2) **(Figure 5h)**, while p-JAK1 and p-JAK3 levels were

unaffected. In conclusion, these findings indicate that DI restrains CD8+ T cell responses, at least in part, by targeting the JAK2-STAT1/3 signaling axis.

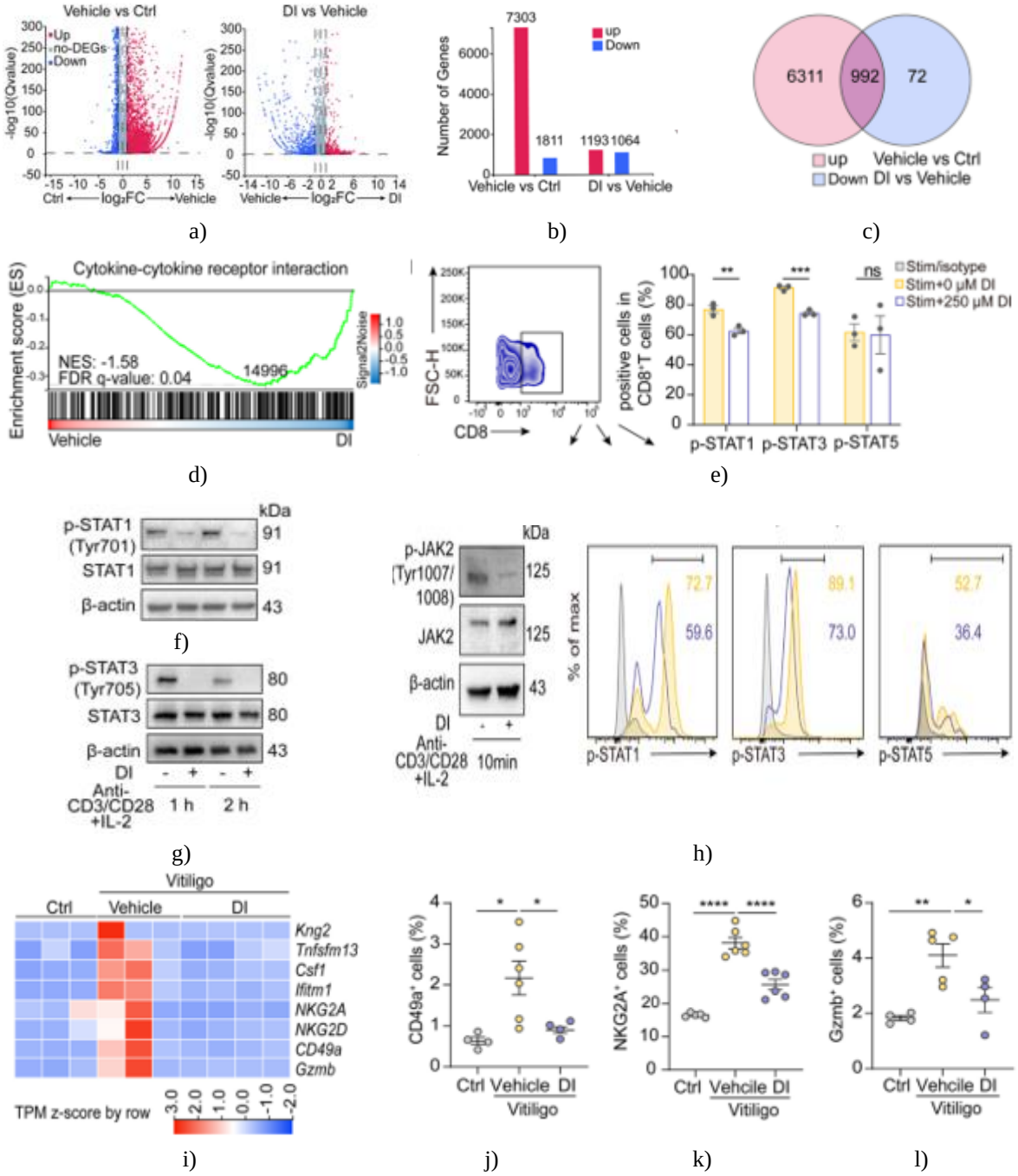

Figure 5. DI blocks JAK-STAT pathway activation and downregulates cytotoxic and inflammatory gene signatures in CD8⁺ T cells.

CD8⁺ T cells were isolated from lymph nodes and subjected to bulk RNA sequencing. Volcano plots (a) and distribution histograms (b) highlight the pattern of differentially expressed genes (DEGs) when comparing vehicle-treated samples from vitiligo mice with either untreated controls or those exposed to DI.

A Venn diagram (c) illustrates the overlap and unique DEGs identified between the DI-treated group and vehicle-treated vitiligo CD8⁺ T cells.

Gene set enrichment analysis (d) revealed significant enrichment of cytokine–cytokine receptor interaction pathway genes when contrasting DI-treated vitiligo CD8⁺ T cells against the vehicle group.

Flow cytometry representative plots and compiled data (e) demonstrated reduced phosphorylation of STAT1, STAT3, and STAT5 in CD8⁺ T cells obtained from vitiligo patients that had been pre-incubated with 250 μM DI.

Western blotting experiments (f, g) confirmed lowered levels of phosphorylated STAT1 and STAT3 (along with total STAT1 and STAT3 proteins) in purified $CD8^+$ T cells from vitiligo patients after the same 250 μM DI pretreatment.

Additional immunoblotting (h) evaluated p-JAK2 and total JAK2 protein abundance in $CD8^+$ T cells pretreated with 250 μM DI followed by 10-minute stimulation.

A heatmap (i) displays the expression patterns of key cytotoxic and proinflammatory genes across $CD8^+$ T cells from control mice, vehicle-treated vitiligo mice, and DI-treated vitiligo mice.

Protein expression of CD49a (j), NKG2A (k), and granzyme B (Gzmb) (l) was quantified by flow cytometry in lymph node $CD8^+$ T cells harvested at week 11 from control, vehicle-treated, and DI-treated vitiligo mice. Results are expressed as mean ± SEM. Statistical analysis employed unpaired two-tailed Student's t-test for panel E and one-way ANOVA followed by Tukey's post-hoc test for panels J–L. Data are representative of at least two independent experiments. ns, not significant; *P < 0.05, **P < 0.01, ***P < 0.001, ****P < 0.0001.

Notably, the markers CD49a, Gzmb, and NKG2D characterize distinct $CD8^+$ T cell populations responsible for executing cytotoxic and proinflammatory activities within vitiligo lesions [44-46]. NKG2A serves as an inhibitory receptor on $CD8^+$ T cells that helps prevent uncontrolled activation while supporting antigen-specific antiviral immunity [47]. Compared with control animals and DI-treated mice, vehicle-treated vitiligo mice exhibited markedly enhanced cytotoxic and proinflammatory features in their $CD8^+$ T cells, reflected by higher transcript levels of Csf1, Ifitm1, CD49a, Gzmb, NKG2D, and NKG2A **(Figure 5i)**. Protein analyses corroborated these findings by showing lowered surface and intracellular expression of CD49a, NKG2A, and Gzmb in the DI-treated group relative to vehicle controls **(Figures 5j–5l)**. In summary, these results demonstrate that DI attenuates the cytotoxic/proinflammatory transcriptional program and compromises the functional capacity of $CD8^+$ T cells.

DI regulates dendritic cell recruitment and activity in vitiligo models both in vivo and ex vivo

Because dendritic cells (DCs) play a pivotal role in initiating and amplifying T cell responses, we examined the impact of DI on DC behavior. In vitiligo mice, there was a substantial rise in epidermal $CD11c^+$ cell numbers, which was substantially reversed upon DI treatment **(Figures 6a and 6b)**. In skin-draining lymph nodes, however, the overall frequency of DCs was reduced in vehicle-treated vitiligo animals compared with both healthy controls and DI-treated vitiligo mice **(Figure 6c)**.

Further subset analysis distinguished migratory DCs ($CD11c^{int}MHCII^{hi}$) from resident DCs ($CD11c^{hi}MHCII^{int}$). DI administration selectively decreased the abundance of migratory DCs **(Figure 6d)**, whereas resident DC populations remained similar across conditions. This pattern indicates that alterations in migratory versus resident subsets do not solely account for the overall decline in lymph node $CD11c^+$ DCs seen in vehicle-treated vitiligo mice.

In the spleen, conventional dendritic cells split into cDC1 ($CD11c^+CD11b^-CD8\alpha^+$) and cDC2 ($CD11c^+CD11b^+CD8\alpha^-$) populations [48]. While cDC1s preferentially drive Th1 polarization and cDC2s promote follicular helper T cell responses [48], the percentages of both splenic subsets were comparable between vehicle- and DI-treated vitiligo mice. Collectively, these data show that DI modifies DC infiltration dynamics across epidermis, spleen, and lymph nodes, with a particular inhibitory effect on the migratory DC compartment in draining lymph nodes.

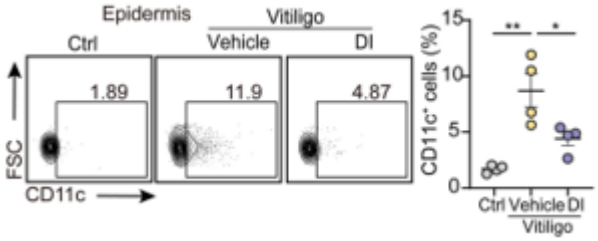

a)

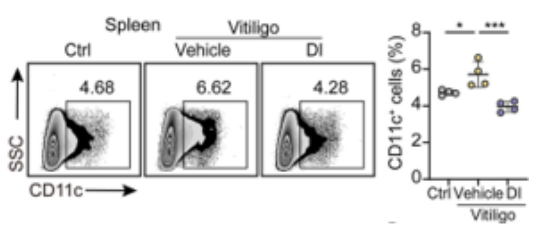

b)

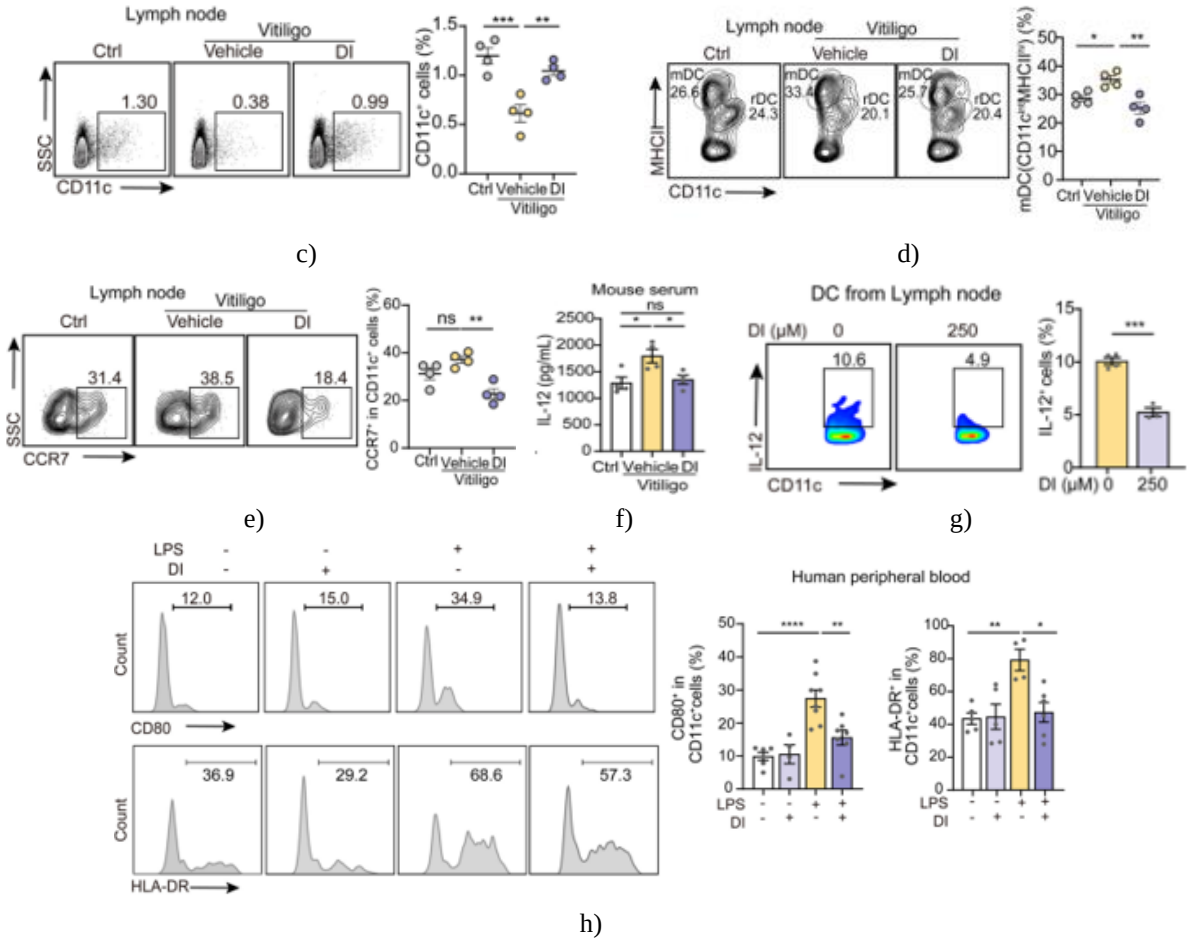

Figure 6. DI restricts dendritic cell infiltration into the epidermis, impairs their migration, and hinders maturation in both living animals and cultured cells.

a–c Flow cytometry representative plots and corresponding quantification of $CD11c^+$ dendritic cells in tail epidermis (a), spleen (b), and lymph nodes (c).

D Representative plots and quantification of migratory $CD11c^{int}MHCII^{hi}$ dendritic cells within lymph nodes at week 11 following the specified treatments.

E Representative flow cytometry plots and quantification of CCR7 expression on $CD11c^+$ cells isolated from lymph nodes of control, vehicle-treated, and DI-treated vitiligo mice at week 11.

F Circulating IL-12 concentrations measured in serum from vehicle-treated and DI-treated vitiligo mice at week 11.

G Flow cytometric assessment of IL-12 production in $CD11c^+$ dendritic cells obtained from lymph nodes of vitiligo mice after pretreatment with or without 250 μM DI.

H Analysis of surface CD80 and HLA-DR expression on $CD11c^+$ dendritic cells from vitiligo patients following ex vivo treatment with 250 μM DI and subsequent stimulation using 1 μg/ml LPS.

Data are presented as mean ± SEM. Statistical evaluations were performed with two-tailed Student's t-test (G) or one-way ANOVA with Tukey's multiple comparison test (A–F, H). All findings are representative of at least two separate experiments. ns, not significant; *P < 0.05, **P < 0.01, ***P < 0.001, ****P < 0.0001.

Additional experiments explored how DI influences dendritic cell trafficking, functional activity, and maturation status. During inflammatory conditions, dendritic cells travel from peripheral tissues to draining lymph nodes through CCR7-mediated chemokine signaling [49]. In lymph nodes of vitiligo mice, DI administration strongly reduced CCR7 levels on $CD11c^+$ cells, indicating impaired dendritic cell chemotaxis **(Figure 6e)**. IL-12 secreted by dendritic cells is essential for promoting Th1 cell differentiation [50]. While IL-12 expression within lymph node dendritic cells remained comparable between vehicle- and DI-treated groups, DI notably lowered the increased serum IL-12 concentrations observed in vitiligo mice **(Figure 6f)**. Consistent with this, exposing cultured vitiligo lymph node cells to DI decreased IL-12 production **(Figure 6g)**. Although CD80 and CD86 levels on dendritic cells were unaffected in lymph nodes at the study endpoint in vivo, ex vivo DI treatment of human

vitiligo-derived dendritic cells suppressed expression of the costimulatory molecules CD80 and HLA-DR, but not CD86, after LPS challenge **(Figure 6h)**. In aggregate, these observations establish that DI limits CCR7-driven dendritic cell migration, curbs IL-12 secretion, and restrains maturation, thereby attenuating dendritic cell-orchestrated immune activation.

Small molecules originating from cellular metabolites hold significant potential for modulating immune cell activity in the treatment of autoimmune disorders [15, 16]. In this work, we identified a new function for the itaconate derivative DI in restraining autoimmune processes through simultaneous control of dendritic cell and $CD8^+$ T cell activities (Additional file 1: Graphical Abstract). Our data show that DI dampens $CD8^+$ T cell effector capabilities by interfering with JAK-STAT signaling, differing from its earlier described actions on macrophages that involve Nrf2 and NF-κB regulation. These results underscore the importance of targeting both dendritic cells and $CD8^+$ T cells as a key approach for managing vitiligo and other similar autoimmune conditions.

Itaconate, generated through metabolic reprogramming in macrophages, exerts important effects in infection control [16], tissue fibrosis [17], and inflammatory regulation [16, 22]. Unlike the minimal concentrations detected in healthy individuals, itaconate levels were elevated in both human patients and mouse models of vitiligo. Because macrophages represent the primary producers of itaconate, we noted expanded macrophage populations in patient blood as well as in mouse lymph nodes during initial disease stages. This points to a link between itaconate elevation and macrophage activation [18] in vitiligo development. Additionally, serum itaconate concentrations were similar between individuals with active and stable vitiligo. The sustained increase likely stems from ongoing macrophage stimulation, as chronic inflammation persists even in stable disease phases [51]. Larger cohort studies will be required to confirm this pattern. Notably, the itaconate concentrations achieved in DI-treated mice (approximately 0.06 μM), **(Figure 2f)** closely matched those measured in vitiligo patients **(Figure 1a)**. Such similarity may arise from species-specific differences in itaconate metabolism, along with variations in body mass, surface area, and compound distribution [52, 53].

We established therapeutic benefits of itaconate and its derivatives using a vitiligo mouse model. Experiments with Acod1 knockout mice demonstrated that lack of itaconate worsened disease progression. Administration of itaconate derivatives elevated blood itaconate and protected melanocytes from immune-mediated destruction. These observations align with protective effects reported in other pathological models, such as elevated itaconate during the acute stage of intracerebral hemorrhage where it exerts beneficial actions [54], consistent with itaconate acting as a broad protective response to diverse stressors. This compensatory immunosuppressive role parallels that of the cytokine IL-10 [55, 56], which rises during both inflammatory and homeostatic states to maintain immune balance and avoid self-tissue injury [56-59].

In a vitiligo model driven by endogenous self-reactive $CD8^+$ T cells, DI curtailed excessive $CD8^+$ T cell activity, broadening its recognized anti-inflammatory profile. DI reduced $CD8^+$ T cell accumulation, cytokine release, and activation within the epidermis, thereby weakening the skin-specific immune attack that directly causes melanocyte loss. In dermal and lymphoid tissues, DI inhibited $CD8^+$ T cell activation and effector functions while leaving overall cell numbers largely unchanged. These patterns indicate that DI primarily disrupts $CD8^+$ T cell functionality across tissues with minimal impact on population size. Complementary ex vivo studies verified that DI directly compromises cytotoxicity, proliferation, and effector activities in $CD8^+$ T cells sourced from both vitiligo mice and human patients. Supporting this, Zhao *et al.* showed that itaconate produced by myeloid-derived suppressor cells limits cytotoxic $CD8^+$ T cell function and thereby weakens anti-tumor responses [60], highlighting shared abilities of DI and itaconate to restrain $CD8^+$ T cell potency. Importantly, the current study reveals that DI's influence on $CD8^+$ T cells occurs independently of itaconate conversion and instead relies on its electrophilic chemical nature. Emerging evidence stresses that DI and itaconate possess distinct properties and must be clearly distinguished [19, 61].

Previous reports indicated that DI or OI dampen macrophage activation via Nrf2 upregulation and NF-κB inhibition, thereby alleviating macrophage-associated pathologies [22, 23, 62]. In contrast to those findings, we uncovered a distinct pathway in which DI inhibits JAK-STAT signaling specifically in vitiligo $CD8^+$ T cells. These cell-type-specific mechanisms may reflect differences in triggering stimuli and downstream targets—macrophages primarily respond through LPS/TLR4 pathways [63], whereas $CD8^+$ T cells depend on TCR/CD3 engagement plus costimulatory signals [64]. Alternatively, varying inflammatory milieus may engage unique transcriptional or metabolic programs across immune cell populations [65-67]. Furthermore, itaconate derivatives can covalently modify cysteine residues or bind specific protein domains to alter target function [21, 68, 69]. Hence, beyond blocking JAK2 phosphorylation, DI may directly modify STAT1 and STAT3 proteins in $CD8^+$ T

cells. Such insights deepen our understanding of JAK-STAT pathway regulation. Overall, these data emphasize DI's context-dependent anti-inflammatory actions across different cell types and disease settings.

This investigation positions DI as a JAK2 inhibitor. Conventional JAK inhibitors often fail to prevent vitiligo recurrence because they do not eliminate skin-resident memory T (Trm) cells [70]. DI may offer additional advantages, as suggested by reports that itaconate and OI decrease $CD103^+$ Trm cell populations in liver models [71]. We propose that DI could selectively act on pathogenic cutaneous Trm cells, providing a more effective means to avert disease relapse. Future studies are warranted to compare DI's performance against standard JAK inhibitors and assess its potential for long-term disease control.

Dendritic cells serve as key activators of $CD8^+$ T cells. Our analyses detected changes in $CD11c^+$ dendritic cell populations across epidermis, spleen, and lymph nodes in vitiligo mice, confirming their participation in melanocyte-targeted immunity. Splenic cDC1 and cDC2 subsets showed no notable differences between treatment groups, suggesting splenic dendritic cells play a limited role in driving T cell responses in this model. In inflammatory settings, skin-resident dendritic cells upregulate MHCII, acquire a mature phenotype, and traffic to lymph nodes via CCR7-dependent migration [72]. These migratory dendritic cells then present antigens to T cells in the nodes [72]. Although CD80/CD86 expression remained unaltered in vivo, DI reduced CCR7 levels and migratory dendritic cell counts, thereby limiting dendritic cell movement. This likely diminishes interactions between dendritic cells and $CD8^+$ T cells in lymph nodes and subsequently restricts $CD8^+$ T cell recruitment to the skin. Furthermore, DI lowered serum IL-12 concentrations in vitiligo mice, matching our ex vivo data showing reduced IL-12 release from lymph node dendritic cells. Thus, DI broadly attenuates dendritic cell contributions—particularly in lymph nodes—by restricting infiltration, migration, and cytokine output. Interestingly, the overall percentage of dendritic cells declined in skin-draining lymph nodes of vehicle-treated vitiligo mice. Possible explanations include dendritic cell apoptosis after engaging with T cells [73, 74] or a relative drop due to expanded total lymphocyte numbers.

Several study limitations should be acknowledged. Yang *et al*. recently demonstrated that CGRP signaling strengthens dendritic cell–$CD8^+$ T cell interactions in vitiligo skin, and blocking this pathway ameliorates disease, underscoring the importance of such crosstalk in pathogenesis [9]. Although our focus centered on separate effects on dendritic cells and $CD8^+$ T cells, we cannot rule out indirect suppression of $CD8^+$ T cells by DI through reduced dendritic cell maturation, cytokine release, and consequent impairment of T cell expansion and activation, or through interference with dendritic cell–T cell contacts. Such dual direct and indirect actions may enable stronger and more comprehensive control of $CD8^+$ T cell responses. Our research emphasizes distinctions between DI and native itaconate but primarily addresses DI's efficacy in vitiligo. Additional head-to-head comparisons will be valuable to clarify relative advantages or disadvantages of each compound in this disease. Our results also indicate that DI promotes repigmentation. To avoid confounding spontaneous recovery, which is uncommon by week 12 in adoptive-transfer vitiligo models [30], we applied DI treatment in a stable model at 24 weeks post-induction. Nevertheless, the precise processes underlying DI-driven repigmentation require further clarification.

Conclusion

In summary, we have established a new therapeutic approach that simultaneously dampens dendritic cell and $CD8^+$ T cell responses to inhibit both the initiation and effector phases of antigen-specific autoimmunity in vitiligo. These findings position DI as a promising therapeutic candidate capable of interrupting vitiligo progression through coordinated regulation of dendritic cells and $CD8^+$ T cells. DI thus emerges as a strong option for improving vitiligo management. As vitiligo represents a prototypical cell-targeted autoimmune disorder with clearly delineated involvement of dendritic cells and $CD8^+$ T cells, strategies simultaneously addressing both populations merit expanded exploration in other autoimmune conditions, including rheumatoid arthritis and multiple sclerosis.

Acknowledgments: None

Conflict of Interest: None

Financial Support: None

Ethics Statement: None

References

1. Ezzedine K, Tannous R, Pearson TF, Harris JE. Recent clinical and mechanistic insights into vitiligo offer new treatment options for cell-specific autoimmunity. J Clin Invest. 2025;135(2). doi:10.1172/JCI185785
2. Wang Y, Li S, Li C. Clinical features, immunopathogenesis, and therapeutic strategies in vitiligo. Clin Rev Allergy Immunol. 2021;61(3):299-323. doi:10.1007/s12016-021-08868-z
3. Chen J, Li S, Li C. Mechanisms of melanocyte death in vitiligo. Med Res Rev. 2021;41(2):1138-66. doi:10.1002/med.21754
4. Xu Z, Chen D, Hu Y, Jiang K, Huang H, Du Y, et al. Anatomically distinct fibroblast subsets determine skin autoimmune patterns. Nature. 2022;601(7891):118-24. doi:10.1038/s41586-021-04221-8
5. van den Boorn JG, Konijnenberg D, Dellemijn TA, van der Veen JP, Bos JD, Melief CJ, et al. Autoimmune destruction of skin melanocytes by perilesional T cells from vitiligo patients. J Invest Dermatol. 2009;129(9):2220-32. doi:10.1038/jid.2009.32
6. Ezzedine K, Eleftheriadou V, Whitton M, van Geel N. Vitiligo. Lancet. 2015;386(9988):74-84. doi:10.1016/S0140-6736(14)60763-7
7. Rosmarin D, Pandya AG, Lebwohl M, Grimes P, Hamzavi I, Gottlieb AB, et al. Ruxolitinib cream for treatment of vitiligo: a randomised, controlled, phase 2 trial. Lancet. 2020;396(10244):110-20. doi:10.1016/S0140-6736(20)30609-7
8. Rosmarin D, Passeron T, Pandya AG, Grimes P, Harris JE, Desai SR, et al. Two phase 3, randomized, controlled trials of ruxolitinib cream for vitiligo. N Engl J Med. 2022;387(16):1445-55. doi:10.1056/NEJMoa2118828
9. Yang X, Ding W, Lou F, Xu H, Sheng A, Sun Y, et al. Nociceptor-derived CGRP enhances dermal type I conventional dendritic cell function to drive autoreactive CD8(+) T cell responses in vitiligo. Immunity. 2025;58(8):2086-103e9. doi:10.1016/j.immuni.2025.05.018
10. Srivastava N, Bishnoi A, Parsad D, Kumaran MS, Vinay K, Gupta S. Dendritic cells sub-sets are associated with inflammatory cytokine production in progressive vitiligo disease. Arch Dermatol Res. 2021;313(9):759-67. doi:10.1007/s00403-020-02168-w
11. Singh A, Das D, Kurra S, Arava S, Gupta S, Sharma A. Dendritic cells and their associated pro-inflammatory cytokines augment to the inflammatory milieu in vitiligo skin. Cytokine. 2021;148:155598. doi:10.1016/j.cyto.2021.155598
12. Mosenson JA, Zloza A, Nieland JD, Garrett-Mayer E, Eby JM, Huelsmann EJ, et al. Mutant HSP70 reverses autoimmune depigmentation in vitiligo. Sci Transl Med. 2013;5(174):174ra28. doi:10.1126/scitranslmed.3005127
13. Okamura K, Arai Y, Kawaguchi J, Tsukada S, Nakamura A, Abe Y, et al. A Hairless Mouse Model for Vitiligo: Enhancing Preclinical Therapeutic Evaluation. J Invest Dermatol. 2025. doi:10.1016/j.jid.2025.06.1596
14. Frisoli ML, Richmond JM, Harris JE. IL-12/IL-23-Independent Function of BATF3-Dependent Dendritic Cells Is Required for Initiation of Disease in a Mouse Model of Vitiligo. J Invest Dermatol. 2024;144(11):2574-7e2. doi:10.1016/j.jid.2024.03.036
15. Zaslona Z, O'Neill LAJ. Cytokine-like Roles for Metabolites in Immunity. Mol Cell. 2020;78(5):814-23. doi:10.1016/j.molcel.2020.04.002
16. Peace CG, O'Neill LA. The role of itaconate in host defense and inflammation. J Clin Invest. 2022;132(2). doi:10.1172/JCI148548
17. Ogger PP, Albers GJ, Hewitt RJ, O'Sullivan BJ, Powell JE, Calamita E, et al. Itaconate controls the severity of pulmonary fibrosis. Sci Immunol. 2020;5(52). doi:10.1126/sciimmunol.abc1884
18. Daly R, Blackburn G, Best C, Goodyear CS, Mudaliar M, Burgess K, et al. Changes in Plasma Itaconate Elevation in Early Rheumatoid Arthritis Patients Elucidates Disease Activity Associated Macrophage Activation. Metabolites. 2020;10(6). doi:10.3390/metabo10060241
19. Swain A, Bambouskova M, Kim H, Andhey PS, Duncan D, Auclair K, et al. Comparative evaluation of itaconate and its derivatives reveals divergent inflammasome and type I interferon regulation in macrophages. Nat Metab. 2020;2(7):594-602. doi:10.1038/s42255-020-0210-0
20. Mills EL, Ryan DG, Prag HA, Dikovskaya D, Menon D, Zaslona Z, et al. Itaconate is an anti-inflammatory metabolite that activates Nrf2 via alkylation of KEAP1. Nature. 2018;556(7699):113-7. doi:10.1038/nature25986

21. Hooftman A, Angiari S, Hester S, Corcoran SE, Runtsch MC, Ling C, et al. The Immunomodulatory Metabolite Itaconate Modifies NLRP3 and Inhibits Inflammasome Activation. Cell Metab. 2020;32(3):468-78e7. doi:10.1016/j.cmet.2020.07.016
22. Bambouskova M, Gorvel L, Lampropoulou V, Sergushichev A, Loginicheva E, Johnson K, et al. Electrophilic properties of itaconate and derivatives regulate the IkappaBzeta-ATF3 inflammatory axis. Nature. 2018;556(7702):501-4. doi:10.1038/s41586-018-0052-z
23. Yi Z, Deng M, Scott MJ, Fu G, Loughran PA, Lei Z, et al. Immune-responsive gene 1/itaconate activates nuclear factor erythroid 2-related factor 2 in hepatocytes to protect against liver ischemia-reperfusion injury. Hepatology. 2020;72(4):1394-411. doi:10.1002/hep.31147
24. Refat MA, Strassner JP, Frisoli ML, Rashighi M, Richmond J, Nada E, et al. Lesional CD8+ T-Cell Number Predicts Surgical Outcomes of Melanocyte-Keratinocyte Transplantation Surgery for Vitiligo. J Invest Dermatol. 2023;143(11):2275-82e6. doi:10.1016/j.jid.2023.03.1689
25. van Geel N, Grine L, De Wispelaere P, Mertens D, Prinsen CAC, Speeckaert R. Clinical visible signs of disease activity in vitiligo: a systematic review and meta-analysis. J Eur Acad Dermatol Venereol. 2019;33(9):1667-75. doi:10.1111/jdv.15604
26. Li S, Kang P, Zhang W, Jian Z, Zhang Q, Yi X, et al. Activated NLR family pyrin domain containing 3 (NLRP3) inflammasome in keratinocytes promotes cutaneous T-cell response in patients with vitiligo. J Allergy Clin Immunol. 2020;145(2):632-45. doi:10.1016/j.jaci.2019.10.036
27. Molodtsov AK, Khatwani N, Vella JL, Lewis KA, Zhao Y, Han J, et al. Resident memory CD8(+) T cells in regional lymph nodes mediate immunity to metastatic melanoma. Immunity. 2021;54(9):2117-32e7. doi:10.1016/j.immuni.2021.08.019
28. Byrne KT, Cote AL, Zhang P, Steinberg SM, Guo Y, Allie R, et al. Autoimmune melanocyte destruction is required for robust CD8+ memory T cell responses to mouse melanoma. J Clin Invest. 2011;121(5):1797-809. doi:10.1172/JCI44849
29. Le Gal FA, Avril MF, Bosq J, Lefebvre P, Deschemin JC, Andrieu M, et al. Direct evidence to support the role of antigen-specific CD8(+) T cells in melanoma-associated vitiligo. J Invest Dermatol. 2001;117(6):1464-70. doi:10.1046/j.0022-202x.2001.01605.x
30. Riding RL, Richmond JM, Harris JE. Mouse model for human vitiligo. Curr Protoc Immunol. 2019;124(1):e63. doi:10.1002/cpim.63
31. Ryan TAJ, Hooftman A, Rehill AM, Johansen MD, Brien ECO, Toller-Kawahisa JE, et al. Dimethyl fumarate and 4-octyl itaconate are anticoagulants that suppress tissue factor in macrophages via inhibition of type I interferon. Nat Commun. 2023;14(1):3513. doi:10.1038/s41467-023-39174-1
32. Xu Z, Chen D, Hu Y, Jiang K, Huang H, Du Y, et al. Anatomically distinct fibroblast subsets determine skin autoimmune patterns. Genome Seq Arch. Available from: https://ngdc.cncb.ac.cn/bioproject/browse/PRJCA006797
33. Yang P, Luan M, Li W, Niu M, He Q, Zhao Y, et al. Single-cell transcriptomics reveals peripheral immune responses in non-segmental vitiligo. Front Immunol. 2023;14:1221260. doi:10.3389/fimmu.2023.1221260
34. Yang P, Luan M, Li W, Niu M, He Q, Zhao Y, et al. Single-cell transcriptomics reveals peripheral immune responses in non-segmental vitiligo. Gene Expression Omnibus. Available from: https://www.ncbi.nlm.nih.gov/geo/query/acc.cgi?acc=GSE231794
35. Li Y, Li S, Duan X, Yang C, Xu M, Chen L. Macrophage Phenotypes and Hepatitis B Virus Infection. J Clin Transl Hepatol. 2020;8(4):424-31. doi:10.14218/JCTH.2020.00046
36. Schmitt H, Ulmschneider J, Billmeier U, Vieth M, Scarozza P, Sonnewald S, et al. The TLR9 agonist cobitolimod induces IL10-producing wound healing macrophages and regulatory T cells in ulcerative colitis. J Crohns Colitis. 2020;14(4):508-24. doi:10.1093/ecco-jcc/jjz170
37. Serrati S, Guida M, Di Fonte R, De Summa S, Strippoli S, Iacobazzi RM, et al. Circulating extracellular vesicles expressing PD1 and PD-L1 predict response and mediate resistance to checkpoint inhibitors immunotherapy in metastatic melanoma. Mol Cancer. 2022;21(1):20. doi:10.1186/s12943-021-01490-9
38. Eberhart T, Stanley FU, Ricci L, Chirico T, Ferrarese R, Sisti S, et al. ACOD1 deficiency offers protection in a mouse model of diet-induced obesity by maintaining a healthy gut microbiota. Cell Death Dis. 2024;15(2):105. doi:10.1038/s41419-024-06483-2
39. ElAzzouny M, Tom CT, Evans CR, Olson LL, Tanga MJ, Gallagher KA, et al. Dimethyl itaconate is not metabolized into itaconate intracellularly. J Biol Chem. 2017;292(12):4766-9. doi:10.1074/jbc.C117.775270

40. Gu M, Zhou X, Sohn JH, Zhu L, Jie Z, Yang JY, et al. NF-kappaB-inducing kinase maintains T cell metabolic fitness in antitumor immunity. Nat Immunol. 2021;22(2):193-204. doi:10.1038/s41590-020-00829-6
41. Noel S, Lee SA, Sadasivam M, Hamad ARA, Rabb H. KEAP1 editing using CRISPR/Cas9 for therapeutic NRF2 activation in primary human T lymphocytes. J Immunol. 2018;200(5):1929-36. doi:10.4049/jimmunol.1700812
42. Luo W, Li YX, Jiang LJ, Chen Q, Wang T, Ye DW. Targeting JAK-STAT signaling to control cytokine release syndrome in COVID-19. Trends Pharmacol Sci. 2020;41(8):531-43. doi:10.1016/j.tips.2020.06.007
43. Philips RL, Wang Y, Cheon H, Kanno Y, Gadina M, Sartorelli V, et al. The JAK-STAT pathway at 30: much learned, much more to do. Cell. 2022;185(21):3857-76. doi:10.1016/j.cell.2022.09.023
44. Gleave A, Granville DJ. Granzyme B in Autoimmune Skin Disease. Biomolecules. 2023;13(2). doi:10.3390/biom13020388
45. Cheuk S, Schlums H, Gallais Serezal I, Martini E, Chiang SC, Marquardt N, et al. CD49a expression defines tissue-resident CD8(+) T cells poised for cytotoxic function in human skin. Immunity. 2017;46(2):287-300. doi:10.1016/j.immuni.2017.01.009
46. Boukhedouni N, Martins C, Darrigade AS, Drullion C, Rambert J, Barrault C, et al. Type-1 cytokines regulate MMP-9 production and E-cadherin disruption to promote melanocyte loss in vitiligo. JCI Insight. 2020;5(11). doi:10.1172/jci.insight.133772
47. Rapaport AS, Schriewer J, Gilfillan S, Hembrador E, Crump R, Plougastel BF, et al. The inhibitory receptor NKG2A sustains virus-specific CD8(+) T cells in response to a lethal poxvirus infection. Immunity. 2015;43(6):1112-24. doi:10.1016/j.immuni.2015.11.005
48. Sulczewski FB, Martino LA, Salles D, Yamamoto MM, Rosa DS, Boscardin SB. STAT3 signaling modulates the immune response induced after antigen targeting to conventional type 1 dendritic cells through the DEC205 receptor. Front Immunol. 2022;13:1006996. doi:10.3389/fimmu.2022.1006996
49. Liu J, Cheng Y, Zhang X, Chen Y, Zhu H, Chen K, et al. Glycosyltransferase Extl1 promotes CCR7-mediated dendritic cell migration to restrain infection and autoimmunity. Cell Rep. 2023;42(1):111991. doi:10.1016/j.celrep.2023.111991
50. Tait Wojno ED, Hunter CA, Stumhofer JS. The immunobiology of the interleukin-12 family: room for discovery. Immunity. 2019;50(4):851-70. doi:10.1016/j.immuni.2019.03.011
51. Shiu J, Zhang L, Lentsch G, Flesher JL, Jin S, Polleys C, et al. Multimodal analyses of vitiligo skin identify tissue characteristics of stable disease. JCI Insight. 2022;7(13). doi:10.1172/jci.insight.154585
52. Nair AB, Jacob S. A simple practice guide for dose conversion between animals and human. J Basic Clin Pharm. 2016;7(2):27-31. doi:10.4103/0976-0105.177703
53. KaruppusamyArunachalam SPS. Bioassays in Experimental and Preclinical Pharmacology. 1st ed. NY: Springer; Humana New York; 2021.
54. Wei C, Xiao Z, Zhang Y, Luo Z, Liu D, Hu L, et al. Itaconate protects ferroptotic neurons by alkylating GPx4 post stroke. Cell Death Differ. 2024;31(8):983-98. doi:10.1038/s41418-024-01303-8
55. Pereira S, Teixeira L, Aguilar E, Oliveira M, Savassi-Rocha A, Pelaez JN, et al. Modulation of adipose tissue inflammation by FOXP3+ Treg cells, IL-10, and TGF-β in metabolically healthy class III obese individuals. Nutrition. 2014;30(7-8):784-90. doi:10.1016/j.nut.2013.11.023
56. Khounlotham M, Kim W, Peatman E, Nava P, Medina-Contreras O, Addis C, et al. Compromised intestinal epithelial barrier induces adaptive immune compensation that protects from colitis. Immunity. 2012;37(3):563-73. doi:10.1016/j.immuni.2012.06.017
57. Nathan C, Ding A. Nonresolving inflammation. Cell. 2010;140(6):871-82. doi:10.1016/j.cell.2010.02.029
58. Nathan C. Nonresolving inflammation redux. Immunity. 2022;55(4):592-605. doi:10.1016/j.immuni.2022.03.016
59. O'Neill LAJ, Artyomov MN. Itaconate: the poster child of metabolic reprogramming in macrophage function. Nat Rev Immunol. 2019;19(5):273-81. doi:10.1038/s41577-019-0128-5
60. Zhao H, Teng D, Yang L, Xu X, Chen J, Jiang T, et al. Myeloid-derived itaconate suppresses cytotoxic CD8(+) T cells and promotes tumour growth. Nat Metab. 2022;4(12):1660-73. doi:10.1038/s42255-022-00676-9
61. Lin J, Ren J, Gao DS, Dai Y, Yu L. The emerging application of itaconate: promising molecular targets and therapeutic opportunities. Front Chem. 2021;9:669308. doi:10.3389/fchem.2021.669308
62. Zhang S, Jiao Y, Li C, Liang X, Jia H, Nie Z, et al. Dimethyl itaconate alleviates the inflammatory responses of macrophages in sepsis. Inflammation. 2021;44(2):549-57. doi:10.1007/s10753-020-01352-4

63. Wu R, Liu J, Wang N, Zeng L, Yu C, Chen F, et al. Aconitate decarboxylase 1 is a mediator of polymicrobial sepsis. Sci Transl Med. 2022;14(659):eabo2028. doi:10.1126/scitranslmed.abo2028
64. Gascoigne NR, Rybakin V, Acuto O, Brzostek J. TCR signal strength and T cell development. Annu Rev Cell Dev Biol. 2016;32:327-48. doi:10.1146/annurev-cellbio-111315-125324
65. Nguyen QP, Takehara KK, Deng TZ, O'Shea S, Heeg M, Omilusik KD, et al. Transcriptional programming of CD4(+) T(RM) differentiation in viral infection balances effector- and memory-associated gene expression. Sci Immunol. 2023;8(83):eabq7486. doi:10.1126/sciimmunol.abq7486
66. Almeida L, Lochner M, Berod L, Sparwasser T. Metabolic pathways in T cell activation and lineage differentiation. Semin Immunol. 2016;28(5):514-24. doi:10.1016/j.smim.2016.10.009
67. Simon-Fuentes M, Herrero C, Acero-Riaguas L, Nieto C, Lasala F, Labiod N, et al. TLR7 activation in M-CSF-dependent monocyte-derived human macrophages potentiates inflammatory responses and prompts neutrophil recruitment. J Innate Immun. 2023;15(1):517-30. doi:10.1159/000530249
68. Chen LL, Morcelle C, Cheng ZL, Chen X, Xu Y, Gao Y, et al. Itaconate inhibits TET DNA dioxygenases to dampen inflammatory responses. Nat Cell Biol. 2022;24(3):353-63. doi:10.1038/s41556-022-00853-8
69. Liao ST, Han C, Xu DQ, Fu XW, Wang JS, Kong LY. 4-octyl itaconate inhibits aerobic glycolysis by targeting GAPDH to exert anti-inflammatory effects. Nat Commun. 2019;10(1):5091. doi:10.1038/s41467-019-13078-5
70. Azzolino V, Zapata L, Jr., Garg M, Gjoni M, Riding RL, Strassner JP, et al. Jak Inhibitors Reverse Vitiligo in Mice but Do Not Deplete Skin Resident Memory T Cells. J Invest Dermatol. 2021;141(1):182-4e1. doi:10.1016/j.jid.2020.04.027
71. Li Y, Li B, Xiao X, Qian Q, Wang R, Lyu Z, et al. Itaconate inhibits CD103 + T RM cells and alleviates hepatobiliary injury in mouse models of primary sclerosing cholangitis. Hepatology. 2024;79(1):25-38. doi:10.1097/HEP.0000000000000549
72. Liu J, Zhang X, Cheng Y, Cao X. Dendritic cell migration in inflammation and immunity. Cell Mol Immunol. 2021;18(11):2461-71. doi:10.1038/s41423-021-00726-4
73. Matsue H, Edelbaum D, Hartmann AC, Morita A, Bergstresser PR, Yagita H, et al. Dendritic cells undergo rapid apoptosis in vitro during antigen-specific interaction with CD4+ T cells. J Immunol. 1999;162(9):5287-98.
74. Ingulli E, Mondino A, Khoruts A, Jenkins MK. In vivo detection of dendritic cell antigen presentation to CD4(+) T cells. J Exp Med. 1997;185(12):2133-41. doi:10.1084/jem.185.12.2133